Desalination and Water Treatment
www.deswater.com

doi: 10.1080/19443994.2015.1048739

57 (2016) 11931–11944
June

Taylor & Francis
Taylor & Francis Group

Fouling reduction of emulsion polyvinylchloride ultrafiltration membranes blended by PEG: the effect of additive concentration and coagulation bath temperature

Mohammad Hossein Davood Abadi Farahani[a], Hesamoddin Rabiee[a], Vahid Vatanpour[b,*], Seyed Mehdi Borghei[a]

[a]*Department of Chemical and Petroleum Engineering, Sharif University of Technology, Azadi Avenue, P.O. Box 11155 9465, Tehran, Iran, Tel. +98 91 26935733; email: mh.farahani89@gmail.com (M.H. Davood Abadi Farahani), Tel. +98 91 27001054; email: hesam.rabiee@ymail.com (H. Rabiee), Tel. +98 21 66164103; email: mborghei@sharif.edu (S.M. Borghei)*
[b]*Faculty of Chemistry, Kharazmi University, Tehran, Iran, Tel./Fax: +98 26 34551023; email: vahidvatanpoor@yahoo.com*

Received 26 September 2014; Accepted 29 April 2015

ABSTRACT

In the present work, ultrafiltration membranes were prepared using emulsion polyvinyl chloride (EPVC) with the addition of various concentrations of polyethylene glycol (PEG) to investigate the morphological structure and separation properties. The effects of polymer concentration, coagulation bath temperature (CBT), and PEG (6 kDa) concentrations—a pore former hydrophilic additive—were studied. Through the phase inversion, the membranes—which were induced by immersion precipitation in a water coagulation bath—were fabricated through dissolving EPVC in N-methyl-pyrrolidinone, a polymer solvent. Morphological features of the membranes were characterized through scanning electron microscopy, pore size and porosity, and contact angle measurements. Water and bovine serum albumin (BSA) were used in order to study the separation and permeation performance of the fabricated membranes at 3 bar, which is operating pressure. The results which were obtained from contact angle test indicated an increment in the membranes hydrophilicity with an increase in PEG concentrations, and then it decreased again. Increasing the CBT led to macrovoid formation in the membrane structure and the appreciation of both membrane permeability and BSA rejection. The addition of PEG resulted in a more porous structure and a higher water flux for those membranes, which were prepared with 13 wt.% EPVC; while, for those which were fabricated with 15 wt.% polymer, an opposite trend was observed.

Keywords: Emulsion polyvinylchloride; Ultrafiltration membrane; Antifouling; Hydrophilicity; Coagulation bath temperature

1. Introduction

Membrane technology is always looking for new compounds for the purpose of inexpensive manufacturing of membranes. The polymers which have adequate mechanical strength, good thermal and chemical resistance, ease of preparation, high efficiency, and high selectivity are suitable for the fabrication of ultrafiltration membranes. During the last decades, UF membranes have been produced by several types of

*Corresponding author.

1944-3994/1944-3986 © 2015 Balaban Desalination Publications. All rights reserved.

polymers such as polysulfone (PS) [1–3], polyethersulfone [4–6], polyetherimide [7], polyvinylidene fluoride [8–10], polyacrylonitrile [11,12], and other polymers. Polyvinyl chloride (PVC) is a polymer that can be produced by three methods of polymerization such as bulk polymerization, suspension polymerization, and emulsion polymerization [13]. The main use of emulsion polyvinyl chloride (EPVC), the PVC which is synthesized by emulsion polymerization method, is manufacturing flexible materials such as artificial leather. EPVC is an excellent polymer because of its incredibly good characteristics, including stiffness, lower price, excellent physical properties and mechanical performance, good thermal stability, and innocuity. In addition, it has strong chemical resistance to the solvents, inorganic acids, halogens, oxidants, and alkalis, all of which are widely used in industries. One of the best advantages of PVC, as a polymer, is its ease of dissolution in common organic solvents such as N-methyl-pyrrolidinone (NMP), N,N dimethylacetamide (DMAc), dimethylformamide (DMF), and tetrahydrofuran (THF). Since PVC is not soluble in water, PVC membranes can be easily fabricated by the phase inversion method [14,15]. The phase inversion method is a well-known technique for the fabrication of asymmetric membranes [16–18], which can be performed by almost all kinds of techniques such as non-solvent-induced phase separation, thermally induced phase separation, vapor-induced phase separation, and evaporation-induced phase separation [10,19]. In these years, research on PVC membranes has focused on the morphological study of the membranes which are fabricated via the phase inversion method.

Xu and Xu [20] have studied the morphology and performance of the hollow fiber membrane which contained PVC, DMAc, water, and additives. They reported that the addition of PVP or PEG, as an additive, increased the membrane porosity and enhanced the permeation due to changing the membrane morphology. However, in their work, antifouling properties were not investigated. Okuno et al. [21] have reported that the fabrication of flat sheet PVC membrane, which is appropriate for pervaporation systems, depends on some factors such as solvents (DMAc, DMF, and THF), degrees of PVC polymerization, PVC concentrations, and additives (water, methanol, ethanol, and *n*-propanol). Bodzek and Konieczny [22] have investigated the effects of molecular mass of PVC, concentration of polymer, and pressure of filtration process on morphology and separation of the UF membranes which are prepared by the combination of PVC, DMF, and water. Hirose et al. [23] have fabricated PVC membranes and discussed the relationship between membrane structures and the phase separation process. Vigo et al. [24] have studied the effect of high frequency discharge on membrane characteristics as a function of discharge time, power and pressure, and the type of gas employed. Peng and Sui [25] have investigated the effect of the increase in hydrophilicity of PVC membranes, caused by blending them with polyvinyl butyral (PVB) as the second polymer. They demonstrated that the addition of PVB can improve the hydrophilic property of the PVC membranes and that the addition of PVC can increase the pore diameter at the bottom of PVB membranes. Babu and Gaikar [26] demonstrated that the effects of blending carboxylated polyvinyl chloride with PVC can result in an increase in transport properties and structural specifications of ultrafiltration membranes. Mei et al. [27] have used PEG, PVP, and small organic molecular sucrose as various additives in PVC/DMAc/water solution systems in order to develop high performance membranes. They studied the effect of the additives on viscosity profile and investigated phase separation behavior of PVC/DMAc polymer solutions at different temperatures. Also, the influence of different additives on the final structure of PVC membranes has been studied by them. In all these studies, the suspension polyvinyl chloride was used. Its properties were improved with additives such as PVP and PEG in order to improve morphology, surface characteristics, performance, and mechanical strength.

In the current study, however, different concentrations of PEG were applied to improve the performance of EPVC as an ultrafiltration membrane. As a novel study, based on its mentioned good characteristics, EPVC rather than SPVC was used in the fabrication of ultrafiltration membranes. The effect of different coagulation bath temperatures (CBTs) on the morphology and performance of the prepared membranes was investigated to reach the best performance. The membrane structure and performance were specified by pure water flux (PWF), porosity and pore size, scanning electron microscopy (SEM), and static water contact angle analyses. Fouling resistance and the rejection of the fabricated membranes were studied, using bovine serum albumin (BSA) as a foulant.

2. Materials and methods

2.1. Materials

EPVC from Arvand Petrochemical Co., Iran, was used as the polymer-forming membrane. Polyethylene glycol (PEG) with 6,000 g/mol molecular weight (Merck) was used as the additive. The solvent used was 1-methyl 2-pyrrolidone (NMP) with an analytical

purity of 99.5% (Merck). Distilled water was used as the non-solvent agent. BSA was obtained from Sigma and used as a foulant.

2.2. Preparation of UF EPVC membranes

The flat sheets of EPVC ultrafiltration membranes were prepared by the phase inversion method via the induced immersion precipitation. The homogeneous blended solutions were prepared by dissolving 13 and 15 wt.% of EPVC polymer at different concentrations of PEG (0–6 wt.%) as a pore former and hydrophilic additive. The compositions and preparation properties of the prepared membranes are presented in Table 1.

The prepared solutions were stirred continuously at around 25˚C until the polymers were completely dissolved in the solvent. When the casting solutions were prepared, which is determined by observing clear solutions, the outcome homogeneous polymer solutions were sonicated for 30 min to remove air bubbles and then were kept away from direct sunlight so as to slow down its aging process for 24 h. Then, the solutions were poured and casted on smooth glass plates, using the Elcometer casting knife with 200 μm thickness. The nascent membranes were instantly immersed in a non-solvent coagulation bath without any evaporation time to complete the phase separation, where the solvent (NMP) and the non-solvent (water) were exchanged. The resulted thin polymeric films were separated from the glass surface within a few seconds. After the main phase separation and membrane formation, the prepared membranes were washed and stored in fresh distilled water for 24 h in surrounding temperature to leach out the remaining solvents and additives completely and to guarantee complete phase separation. As an ultimate stage, the membranes were placed between two sheets of filter papers for 24 h at room temperature for drying.

2.3. Characterization of the membranes

2.3.1. Scanning electron microscopy

The cross-sectional morphology of the fabricated membranes was inspected, using a VEGA ‖ (TESCAN, Czech Republic) SEM with magnification of 1,000 and 5,000. All of the samples were sputter-coated with a thin layer of gold to minimize sample charging. SEM images were taken under very high vacuum conditions, operating at 20 kV.

2.3.2. Contact angle

Deionized water was used as the probe liquid in order to specify the hydrophilicity at the membrane surface. The images of 3 μl deionized water droplets on the membrane surface were obtained, using OCA20, Dataphysics Instruments, Germany, which are taken at 25˚C with a relative humidity of 50%. Equilibrium sessile drop contact angles were determined by the steady-state angles, which were typically observed to gain a constant value between 30 and 120 s after the drop had contacted the membrane surface. At least, five measurements were taken at different locations on the membrane surface to determine the average contact angle value.

2.3.3. Water permeation experiments

The evaluations of PWF and protein rejection were performed, using a dead-end membrane cell, as was shown in our previous article [28], which had a

Table 1
Compositions and preparation conditions of EPVC UF membranes

	Solution compositions		
Membrane code	Polymer EPVC wt.%	PEG 6000 wt.%	CBT (˚C)
13E, 0P	13	0	25
13E, 2P	13	2	25
13E, 4P	13	4	25
13E, 6P	13	6	25
15E, 0P	15	0	25
15E, 2P	15	2	25
15E, 4P	15	4	25
15E, 6P	15	6	25
13E, 4P, 5T	13	4	5
13E, 4P, 45T	13	4	45

membrane effective area of 19.6 cm^2. Before measurements, all the membranes were pretreated and compacted at the high pressure difference of 4 bar for 30 min. Then, the PWF tests were conducted at an operation pressure of 3 bar. The permeates were collected and weighed over a given period. The water flux (J), whose unit is "kg/m^2 h", was calculated, using Eq. (1):

$$J = \frac{M}{A\,\Delta t} \tag{1}$$

where M (kg) is the mass of permeated water, A (m^2) is the membrane area, and Δt (h) is the permeation time. The experiments were carried out at 25 ± 1°C.

2.3.4. Analysis of membrane fouling resistance

For the analysis of the membrane fouling resistance, after water flux tests, the stirred cell was rapidly refilled with 500 mg/l BSA solution (pH 7.0 ± 0.1). The flux for protein solution, J_p (kg/m^2 h), was measured based on the permeate quantity leaking from the membranes at 3 bar for 90 min.

For concentration evaluation of the permeated BSA, UV absorbance of the permeates was measured at 280 nm. The percentage of BSA rejections (R) was evaluated by Eq. (2), where C_p (ppm) and C_F (ppm) were the BSA concentration in permeate and feed solutions, respectively. There is very little difference between the initial and final volume of the BSA solutions in the cell. Also, the BSA concentration in the permeate, as compared to the feed, is very low. In this regard, using Eq. (2) is an appropriate way to calculate the rejection of the BSA.

$$R\,(\%) = \left(1 - \frac{C_p}{C_F}\right) \times 100 \tag{2}$$

After the filtration of BSA solution, membranes were removed from the stirred cell and washed with distilled water. The membranes were initially rinsed, and then they were submerged in distilled water for 30 min. This was followed by the measurement of water flux of the cleaned membranes $J_{w,2}$ (kg/m^2 h). The flux recovery ratio (FRR) was calculated by the following equation, where $J_{w,1}$ (kg/m^2 h) is the first water flux:

$$\mathrm{FRR}\,(\%) = \left(\frac{J_{w,2}}{J_{w,1}}\right) \times 100 \tag{3}$$

$J_{w,1}$ and $J_{w,2,}$ which were used as the flux of membranes, are stable fluxes. Generally, higher FRR indicates a better antifouling property of the prepared membrane.

2.3.5. Porosity and pore size

Using the gravimetric method, the membranes overall porosity (ε) was calculated as follows [29]:

$$\varepsilon = \frac{w_1 - w_2}{A \times l \times d_w} \tag{4}$$

where w_1 and w_2 (g) are the weights of the wet and dry membranes, respectively. l (m) is the membrane thickness, A (m^2) is the membrane area, and d_w is the water density (0.998 g/cm^3). First, in order to make sure that all the pores of the membranes are filled with water, a certain piece of membrane is immersed in distillated water for at least 12 h. Shortly after that, the sample was supposed to be weighed just after the water on the surface of the samples is cautiously cleaned. Afterwards, the samples are placed in an oven for 2 h at 60°C to let the water evaporate from membrane pores and be weighed again. Concerning this, to calculate the porosity of membranes, we can use Eq. (4).

Mean pore radius (r_m, nm) of the membranes was also measured by the Guerout–Elford–Ferry equation, as follows [29]:

$$r_m = \sqrt{\frac{(2.9 - 1.75\varepsilon) \times 8\eta l Q}{\varepsilon \times A \times \Delta P}} \tag{5}$$

where Q (m^3/s) is the water flux, η is the water viscosity (8.9×10^{-4} Pa s), and ΔP is the operation pressure (0.3 MPa).

3. Results and discussion

3.1. Characterization and morphology of EPVC membranes

3.1.1. Effects of PEG on membrane morphology

SEM images were taken in order to visualize the effects of PEG concentrations, as an additive, on membrane morphology. It is important to mention that the SEM observation for the membrane surface was repeated at least four times for every membrane, and similar images were obtained for all the samples.

A morphological characteristic of an asymmetric membrane consists of a dense top layer and a porous sub layer with a finger-like structure, both of which

were observed for all of the membranes. The dense top layer is responsible for the permeation and rejection of solutes, while the sub layer plays a role as a mechanical support. The phenomena behind the formation of this typical structure had been explained in quite a few previous publications [30,31].

Figs. 1 and 2 illustrate SEM cross-sectional images of the prepared membranes—13 wt.% EPVC, 0–6 wt.% PEG, and 15 wt.% EPVC, 0–6 wt.% PEG—respectively. By observing these images, it becomes obvious that, when PEG concentration is increased, macrovoids develop in number and size, promoting the formation

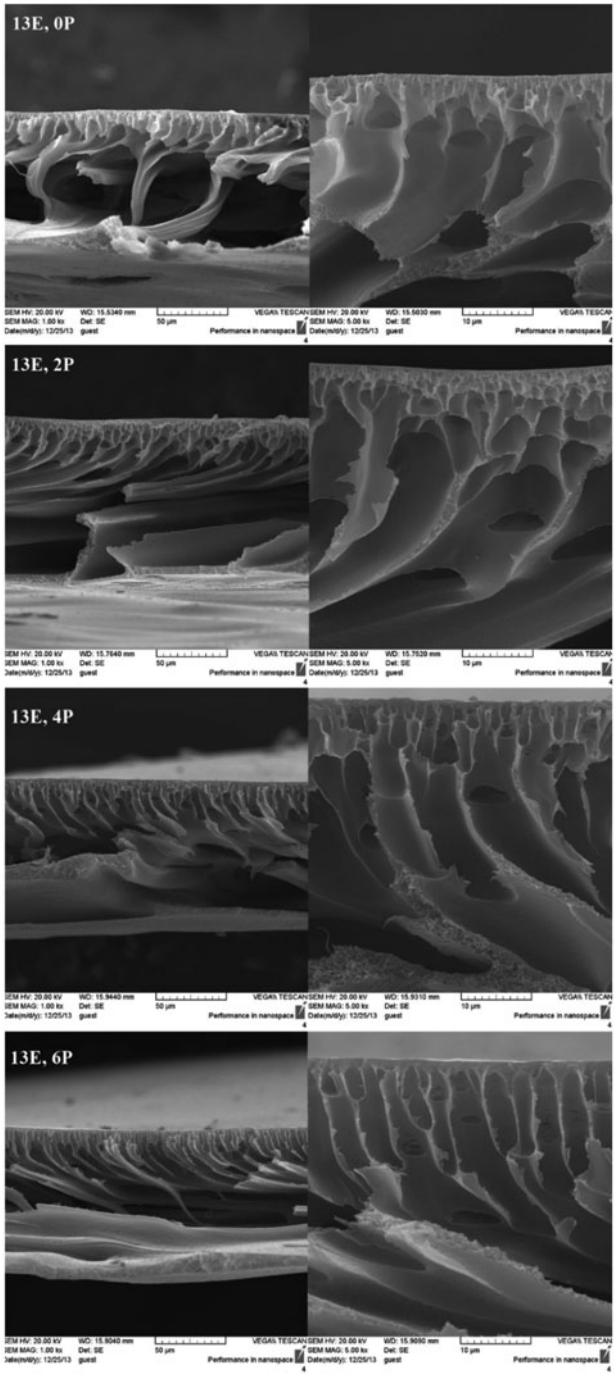

Fig. 1. The SEM cross-sectional images of the 13 wt.% EPVC membranes.

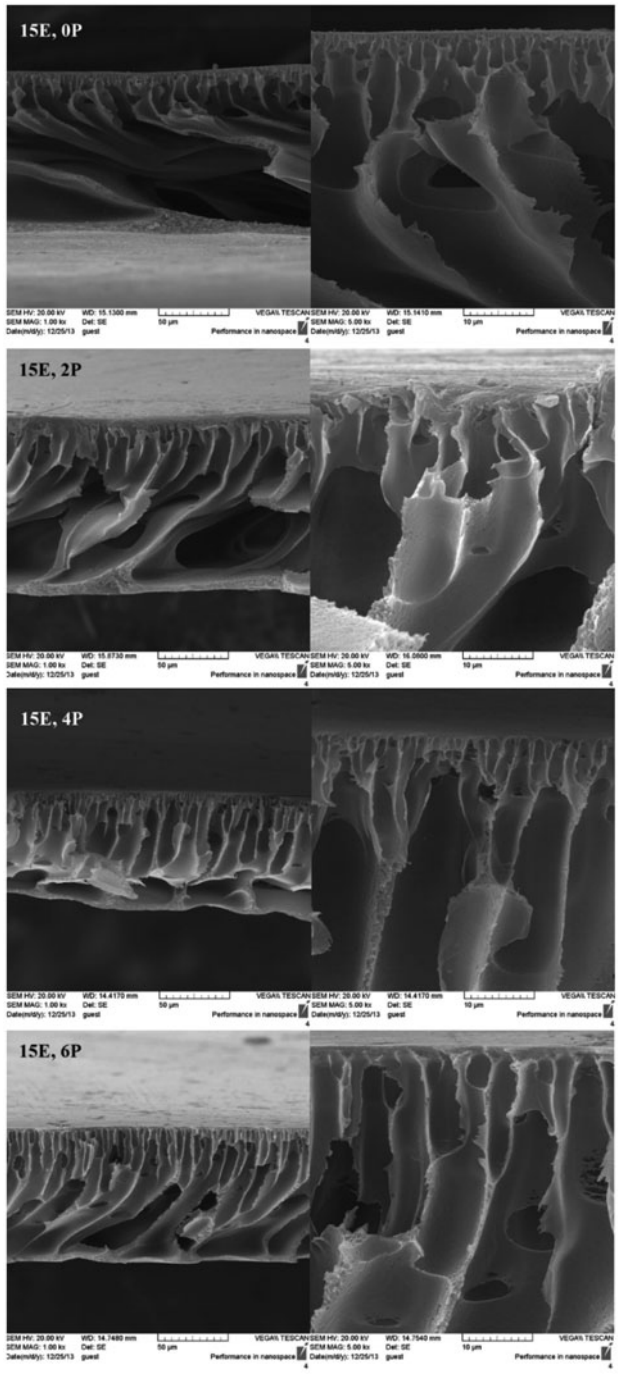

Fig. 2. The SEM cross-sectional images of the 15 wt.% EPVC membranes.

of many finger-like pores. The finger-like pores gradually lengthened to the bottom of the membranes at higher concentrations of PEG, which results in membranes with more porosity. Similarly, Kim and Lee [32] have shown that, the bigger the PEG/NMP ratio becomes, the greater the pore size of the top surface gets, the more porous the top layer becomes, and the larger the distance from the top surface to the starting point of the macrovoid formation will be.

According to Fig. 1, it can be perceived that, at constant CBT (25˚C), for 13 wt.% EPVC, the increase in PEG concentration from 0 to 6 wt.% leads to the formation of more finger-like structures and porous structures on the surface of the membranes. As was observed, the membrane prepared with no PEG in their casting solution has a thicker dense top layer.

Fig. 2 shows that, at constant CBT (25˚C), for 15 wt.% EPVC, increasing PEG concentration from 0 to 6 wt.% leads to the development of more finger-like structures. Also, it can be realized that increasing PEG concentration from 0 to 6 wt.% results in the formation of a denser structure on the top layer of the membrane.

The results which appeared suggest that the addition of the PEG in different concentrations may be used to prepare a desired membrane for ultrafiltration.

The comparison between SEM images related to 13 wt.% EPVC and 15 wt.% EPVC shows that increasing 2 wt.% in EPVC concentration leads to a change in the skin layer structure from dense to finger-like. Also, the sub layer changed from macrovoid to a finger-like structure.

Fig. 3 demonstrates the comparison between surface images of "13E, 0P" and "13E, 4P" membranes. It can be concluded that the 13E, 4P membrane had a larger pore size than 13E, 0P. Apart from this, it can be seen that the pore density of the 13E, 4P membrane is higher than that of the 13E, 0P membrane. The pores on the top of the surfaces seem to be unclear, but the roughness of 13E, 0P partly increases with the addition of 4 wt.% PEG. Generally, it can be said that the pore size of the membrane depends upon the size of such congregated particles as macromolecules, piles, or pile congregated [33,34]. Increasing the pore size can be roughly estimated from the increase in the roughness and size of the congregated particle which is observed at the top surface. This analysis seems to be reasonable if it agrees well with the permeation results, which can be influenced not much by the top layers in asymmetric structures. As to the membrane morphologies, the porosity of the top layer is closely related to the macrovoid formation. When a more porous top layer is created, the macrovoids formation is largely suppressed. The more porous top layer needs a larger distance from the top surface to the starting point of macrovoids in order to limit the large non-solvent inflow to the sub layer, because a large non-solvent inflow induces many nuclei formation in the sub layer, thereby preventing the macrovoids formation [32].

3.1.2. Effects of CBT on the morphology of the EPVC membrane

The effects of three different levels of CBT (5, 25, and 45˚C) on the membranes morphology for the best characterized membrane—that is—"13E, 4P", are illustrated in Fig. 4. It is generally accepted that the instantaneous demixing leads to the creation of a macrovoid structure, while the postponed demixing

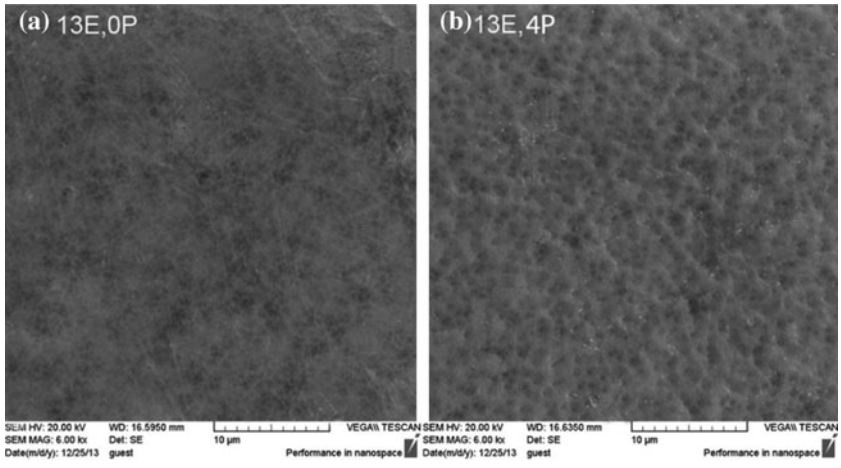

Fig. 3. The SEM surface images of 13 wt.% EPVC membranes with (a) 0 wt.% PEG and (b) 4 wt.% PEG.

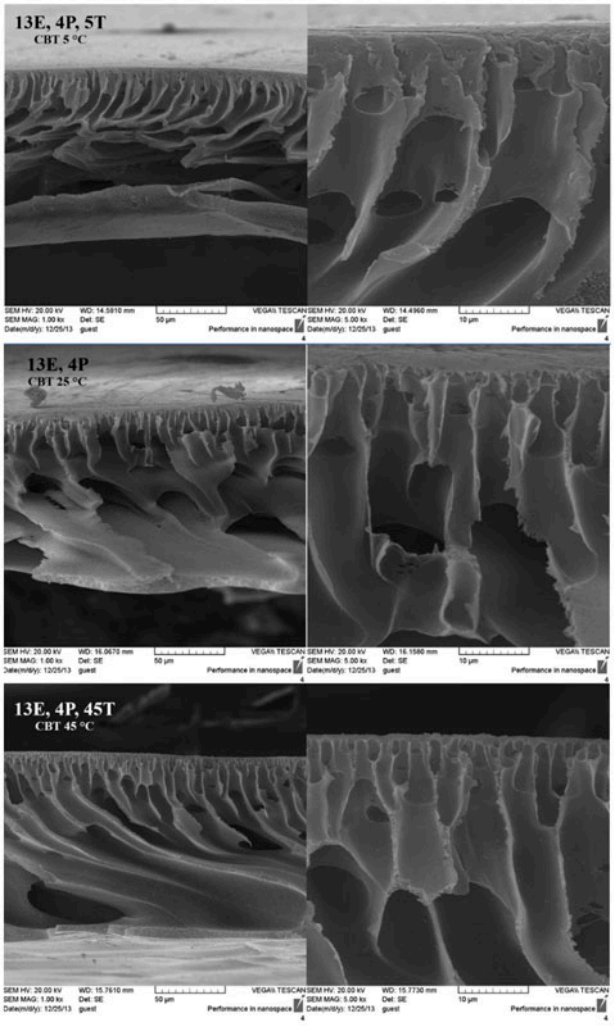

Fig. 4. The SEM cross-sectional images of the "13E, 4P" various CBT membranes.

leads to a sponge-like structure in the cross section images [35]. As was observed in the cross-sectional SEM images of the membrane, which is prepared at 5℃, it has an asymmetric structure with bigger macropores in its sub layer. In comparison to the cross-sectional SEM images of the skin layer of the membranes that are prepared at various levels of CBT, it is perceived that the membrane prepared at 5℃ CBT has a denser skin layer. Increasing the CBT from 5 to 25℃ results in the appreciation of the size of the surface pores of the membrane. By doing so, the structure of the sub layer of the membrane changes from macrovoid to fully developed finger-like pores. Generally, the formation of microvoids occurs under quick precipitation conditions, which occurs faster at higher temperatures [36]. Concerning the slow demixing, nucleation happens after a certain period of time. By so doing, polymer concentration increases in the top layer of the membrane. Then, nucleation starts in the minor layer at a short time period. Accordingly, the composition and size of the nucleus in the former layer is similar to the new nucleuses, which are gradually formed in their proximity [37]. In other words, in slow demixing, the high-handedly growth of the limited nucleuses is prevented on the top layer, as a result of which, a large number of small nucleuses are created and distributed all over the polymer film. As a result, opposite to instantaneous demixing, the formation of macrovoids is repressed, and denser membranes are created as well. Increasing CBT to 45℃ dramatically increases bilateral diffusivities between the solvent (NMP) and non-solvent (water) in the casting solution during the solidification process of polymeric film. After the immersion of the casting solution into the distilled water bath, this phenomenon rapidly limited the growth of the nucleuses and prevented their formation quickly. This results in the formation of a few numbers of large nucleuses in each part of the casting solution [36,38]. As is shown in the cross-sectional SEM images, the membrane which is fabricated at 45℃ CBT has big macrovoids in its structure. These observations are in agreement with the report mentioned in the literature [35].

3.2. Permeation, antifouling, and rejection characteristics of EPVC UF membranes

3.2.1. PWF of the membranes

The presence of PEG as an additive in the casting solution had a significant effect on water permeability of the membranes. As is shown in Fig. 5, for those membranes which have 13 wt.% EPVC in their casting solutions, the appreciation of PEG concentration from 0 to 6 wt.% resulted in the growth in the amount of

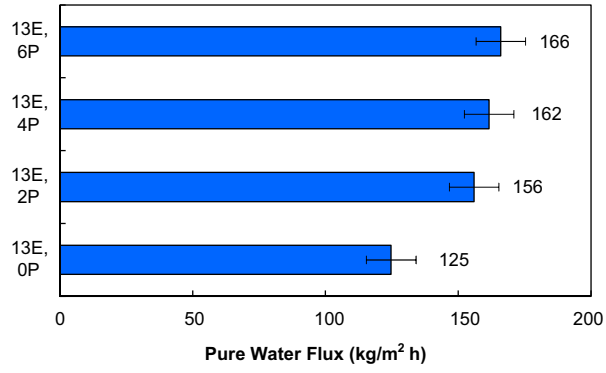

Fig. 5. PWF of the prepared 13 wt.% EPVC membranes with different concentrations of PEG.

water permeability. As is shown in SEM images (Fig. 1), increasing the PEG concentrations result in the formation of a more finger-like structure on the top layer of the membranes, which can lead to an increase in the PWF. However, the membranes containing 15 wt.% EPVC in their casting solutions showed an opposite trend. Based on Fig. 6, with increasing PEG concentration from 0 to 6 wt.%, the PWF decreased. As can be seen in Fig. 2, although increasing the PEG concentrations improved the formation of finger-like structures, the formation of a denser structure on the top layer of the membrane led to decreasing the PWF. In high concentrations of EPVC, the addition of PEG polymeric additive may increase the casting solution viscosity to reach the critical area of polymeric solution that caused the reduction of diffusional exchange rate between the solvent (NMP) and non-solvent (water) during the solidification process, thus hindering instantaneous demixing in the phase separation technique and decreasing the PWF. This phenomenon led to delayed demixing, and as a result, to the formation of a denser structure [39].

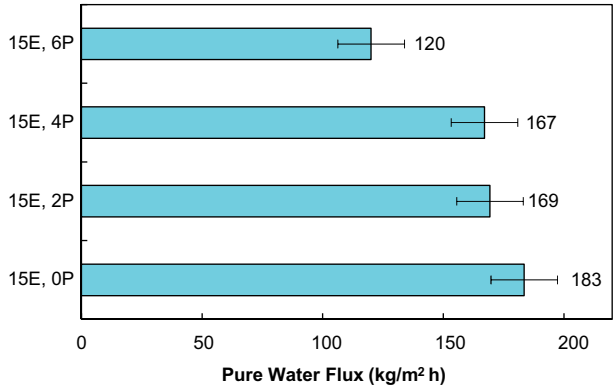

Fig. 6. PWF of the prepared 15 wt.% EPVC membranes with different concentrations of PEG.

Membrane hydrophilicity and morphology are the two main parameters which can affect the permeation flux [40]. It is clear that, with modifying the membrane material or changing it to a hydrophilic one, the permeation flux increases [41]. Also, by increasing membrane pore size and porosity and by developing a finger-like structure, the permeability of membranes is enhanced [40,42].

The hydrophilicity of the surface of membrane can be analyzed by water contact angle measurement. A lower contact angle indicates that the membrane surface is more hydrophilic in nature. It should be noted that PEG is more hydrophilic in comparison with EPVC, and consequently its presence in the membrane structure increases the membrane hydrophilicity. Figs. 7 and 9 depict the static contact angle of the prepared membranes. As can be observed in Fig. 7, for 13 and 15 wt.% EPVC membranes, the contact angle declined significantly with the increase in PEG concentrations from 0 to 4 wt.% into the casting solution and then increased with increasing PEG concentration from 4 to 6 wt.%. The 13E, 0P membrane showed the highest water contact angle, 70.4˚. For the 13E, 4P membrane, the water contact angle reduced to 60.3˚.

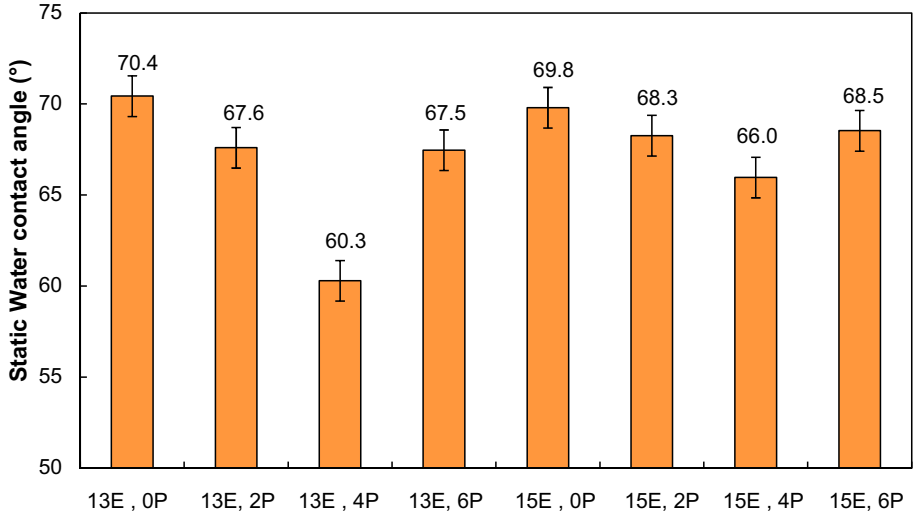

Fig. 7. Static water contact angle of the EPVC membranes in the 25˚C CBT (average contact angle of five replicates are reported).

Fig. 8 shows the changes in the PWF of membranes with altering the CBT. As was mentioned above and according to the SEM images presented in Fig. 4, an increase in CBT always increases membrane porosity. Thus, the mentioned increase in PWF can be related to membrane porosity and hydrophilicity. According to Fig. 9, increasing CBT form 5 to 25˚C resulted in a lower contact angle, and consequently, in higher membrane hydrophilicity. The membrane which is prepared at the highest temperature, that is, 45˚C, showed the highest contact angles. The molecular weight of PEG employed in this work was not very low, and consequently it cannot be completely washed out during the formation of the membranes [42]. Thus, it can be expected that some of the PEG is entrapped in the membrane structure in general and in the membrane pores in particular. The quantity of the residual PEG, which has a direct relationship with the membrane hydrophilicity, highly depends on CBT. At higher CBTs, particularly at 45˚C, because of higher solubility and diffusivity of PEG, it can be more easily washed out with the solvent during the membrane formation process. In this regard, the phenomenon resulted in a higher contact angle because of the reduction of the membrane hydrophilicity.

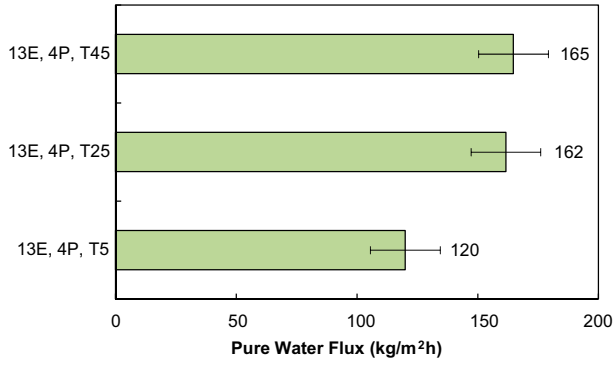

Fig. 8. PWF of the "13E, 4P" various CBT membranes.

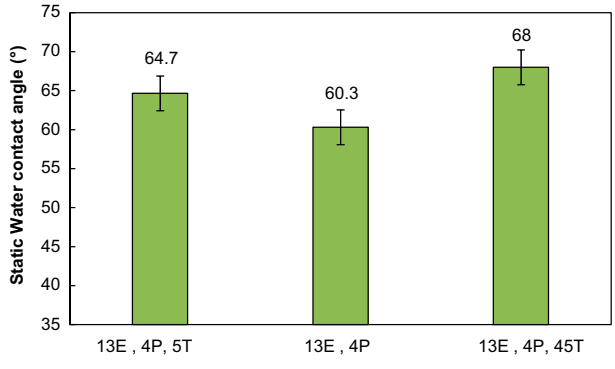

Fig. 9. Static water contact angle of the "13E, 4P" various CBT membranes (average contact angle of five replicates are reported).

The growing trend of PWF, by increasing the CBT presented in Fig. 8, revealed that the intensive reduction of the membrane hydrophilicity (an increase in the contact angle) in 45˚C did not reduce the membrane permeability. This phenomenon indicates that the structure of the prepared EPVC membrane has more influence than hydrophilicity does. Concerning this, the role of porosity and morphology is pretty important. Also, the intensive increasing trend of PWF with increasing CBT from 5 to 25˚C can lead to a change in the membrane structure and porosity (Fig. 4) and to the increasing membrane hydrophilicity.

There is an important parameter, porosity of the membranes. As is shown in Table 2, with an increase in PEG concentration, the porosity of the membranes increased. There is an agreement on this observation and literature [20]. One of the advantages of increasing porosity is flux enhancement. As is reported in Fig. 5, an increase in porosity led to the flux enhancement. However, increasing porosity for those membranes that have 15 wt.% EPVC in their casting solution, led to a decline in flux. This unexpected phenomenon, as we mentioned, can be attributed to the formation of a denser structure on the top layer of the membranes because of high concentrations of EPVC/PEG polymer. An increase in CBT led to increasing porosity of the membranes, for the formation of microvoids which occurs faster at the higher temperatures [36].

On the parameters that have effect on FRR is mean pore radius of the membranes. The "13E, 4P, 45T" membrane has a mean pore radius of 13.4 (±0.9), and it shows the fouling capability of the membrane. This is because of the entrapping of the foulant molecules

Table 2
Porosity and mean pore size of the UF membranes

Membrane	Porosity (%)	Mean pore radius, r_m (nm)
13E, 0P	70.7 (±3.3)	12.3 (±0.5)
13E, 2P	76.9 (±3.5)	10.9 (±0.6)
13E, 4P	78.3 (±3.8)	10.1 (±0.7)
13E, 6P	80.2 (±4.1)	12.5 (±0.9)
15E, 0P	64.9 (±3.4)	12.9 (±0.8)
15E, 2P	66.9 (±3.5)	11.8 (±0.6)
15E, 4P	68.5 (±3.2)	9.1 (±0.6)
15E, 6P	72.7 (±3.1)	8.9 (±0.7)
13E, 4P, 5T	68.3 (±3.4)	11.5 (±0.6)
13E, 4P, 45T	82.6 (±4.0)	13.4 (±0.9)

in the pores of the membrane. A change in pore radius can affect fouling capability.

3.2.2. Evaluation of antifouling properties

Fouling is a major obstacle concerning hydrophobic membranes such as EPVC. It leads to the interaction between the membrane surface and the foulant. Fouling results in a decline in flux or an increase in applied pressure, and reduces membrane life time as well. Therefore, the reduction of the membrane fouling is one of the main aims of the researchers [14].

Figs. 10 and 11 show the flux of membranes during three steps: pure water permeation, BSA filtration,

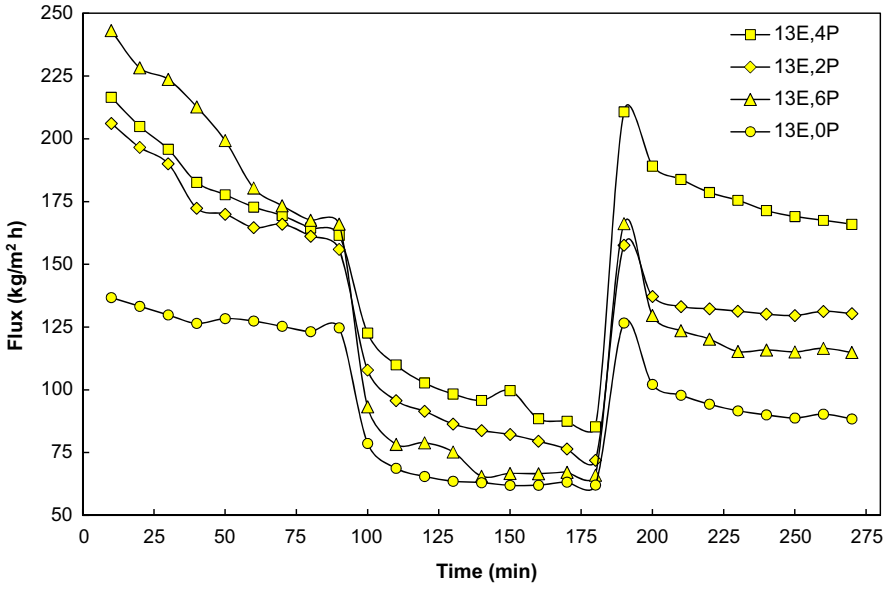

Fig. 10. Flux vs. time for 13 wt.% EPVC membranes at 3 bar during three steps: PWF for 90 min, BSA solution (500 ppm, pH 7 ± 0.1) flux for 90 min, and water flux after 30 min washing with pure water for 90 min.

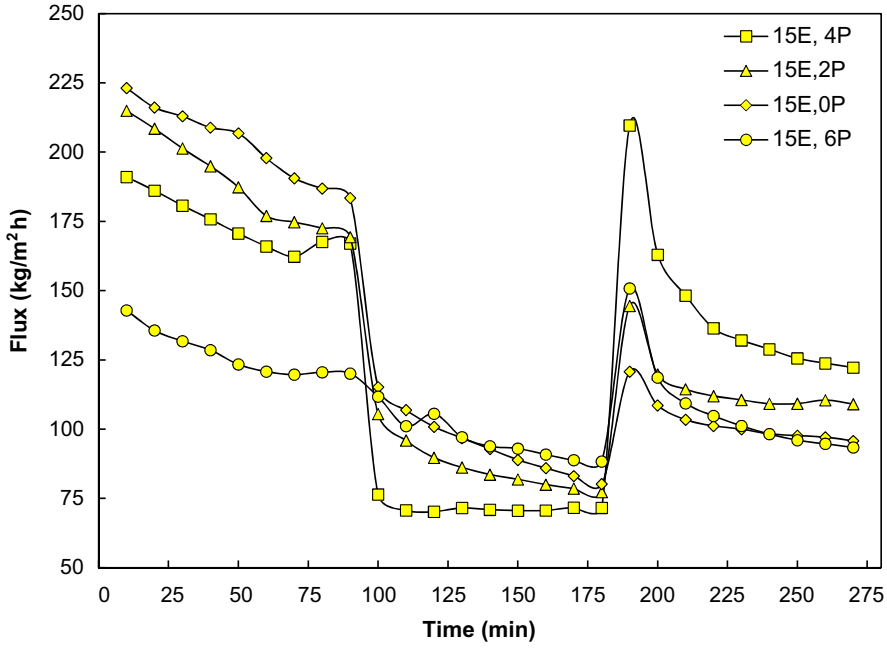

Fig. 11. Flux vs. time for 15 wt.% EPVC membranes at 3 bar during three steps: PWF for 90 min, BSA solution (500 ppm, pH 7 ± 0.1) flux for 90 min, and water flux after 30 min washing with pure water for 90 min.

and PWF after membrane washing. Although all membranes showed similar trends of BSA flux decline, the decline in the BSA flux for the 13 wt.% EPVC membranes was seen less when the increase in PEG concentration is up to 4 wt.%, and the least decline of BSA flux for the 15 wt.% EPVC membranes was seen in 15E, 6P membrane.

The BSA rejection value of the membranes is shown in Fig. 12. All of the prepared membranes had a BSA rejection of more than 96%. The EPVC membrane which contained no additive had the highest protein rejection, while the membranes which had an additive in their casting solutions showed a lower protein rejection.

The fouling resistance ratio (FRR) demonstrates antifouling property of the membranes. Fig. 13 shows that 13E, 6P and 13E, 0P membranes with 69 and 71%, respectively, had a low FRR value, while maximum FRR belonged to the 13E, 4P with the mean value of 103%.

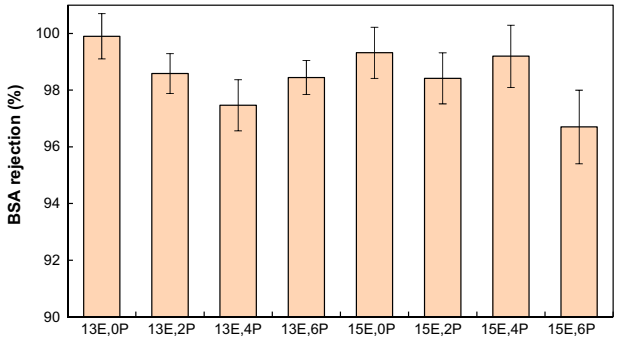

Fig. 12. BSA rejection of EPVC membranes.

It can be concluded that the antifouling capability of EPVC membrane was significantly improved with an increment in PEG concentration. This phenomenon was attributed to the increased surface covering of hydrophilic groups, which can create a denser and more stable hydration layer. The hydrophilic groups on the surface of EPVC–PEG membranes are the result of the addition of PEG, which decreases the affinity between the membrane and the foulant and weakens the interactions between the protein molecules and the membrane surface. This would in turn result in easily washing the membrane surface, thus contributing high recyclability to the membranes.

As an exception, the antifouling properties (FRR) of the 13E, 6P membrane was lower than those of all the membranes which contain 13 wt.% EPVC. It is due to the lower hydrophilicity of this membrane, which is the most important parameter in controlling the antifouling characteristics of ultrafiltration membranes. This observation is consistent with the high water contact angle of 13E, 6P membrane.

Fig. 13 demonstrates the increase in FRR with increasing PEG concentration in 15 wt.% EPVC membranes. Raising PEG concentration increases membrane hydrophilicity that is in contact with the aqueous phase, weakening the interactions between the protein molecules and the membrane surface. This phenomenon results in the ease of washing the membrane surface, thus contributing high recyclability to the membranes.

Fig. 14 shows the effect of CBT on PWF, the flux of BSA solution, and BSA fouling condition. By an increase in CBT, the PWF increases. An increase in CBT from 5 to 25˚C led to 35% increase in PWF, while

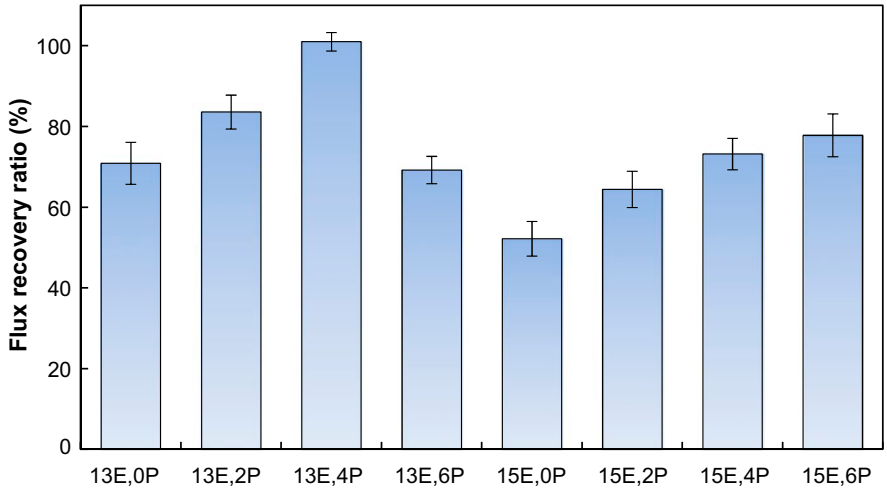

Fig. 13. FRR of prepared EPVC membranes after BSA fouling.

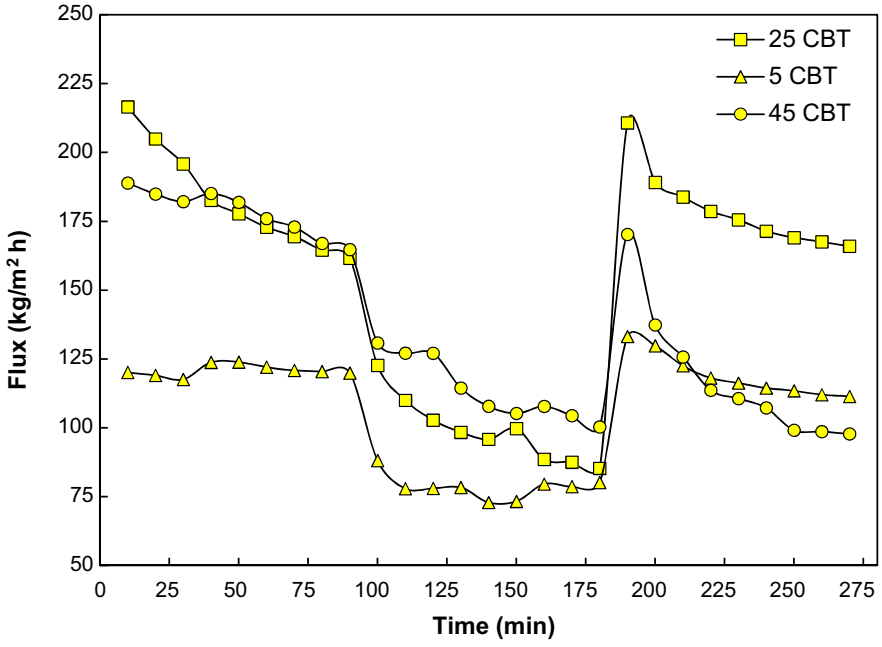

Fig. 14. Flux vs. time for the "13E, 4P" various CBT membranes at 3 bar during three steps: PWF for 90 min, BSA solution (500 ppm, pH 7 ± 0.1) flux for 90 min, and water flux after 30 min washing with pure water for 90 min.

increasing CBT from 25 to 45˚C CBT resulted in 2% PWF enhancement. This comparison indicates that with increasing CBT, the enhancement rate of PWF declined. The membrane which prepared at 5˚C showed the lowest BSA solution permeation, but, its flux recovery is higher than the membrane, which prepared at 45˚C.

Fig. 15 illustrates the BSA rejection for the "13E, 4P" membranes which were prepared in various CBTs. The BSA rejections for all the membranes are above 95%. The rejection enhances to almost 97.5% for the membrane which fabricated in 25˚C CBT. A

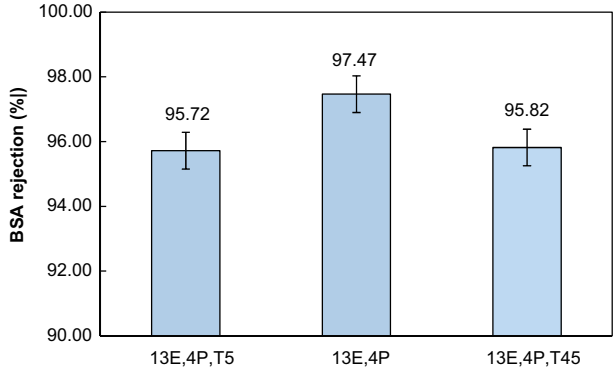

Fig. 15. BSA rejection of the "13E, 4P" membranes in various CBT.

change in CBT from 25 to 45˚C led to a decrease in BSA rejection of membranes because of increasing mean pore radius and a decrease in residual PEG in the structure of the membrane. As to a change in CBT from 5 to 25˚C, it is clear that a decrease in mean pore radius resulted in the enhancement of BSA rejection. An increase in the mean pore radius led to increasing membrane fouling because of the ease of entrapping foulant materials in a bigger pore of the membranes.

Apart from this, the BSA rejection can attributed to hydrophilicity of the membranes. As is presented in Fig. 9, it can be perceived that a change in hydrophilicity of the membrane can directly affect the BSA rejection and other fouling parameters. Concerning a hydrophilic membrane, there is a weak interaction between foulant and the surface of the membrane, leading to better fouling characteristics.

Fig. 16 represents FRR parameter for the "13E, 4P" membranes which were prepared in various CBTs. According to this figure, maximum FRR belongs to the "13E, 4P" membrane that is fabricated in 25˚C CBT. As mentioned, the quantity of residual PEG in membrane, which has a direct relationship with the membrane hydrophilicity (Fig. 8), highly depends on the CBT. It can be expected that with an increase in CBT, the quantity of the PEG that is washed out from the membrane during formation process increases. Therefore, the lowest value of FRR for the "13E, 4P, 45T" membrane is due to decreasing hydrophilicity,

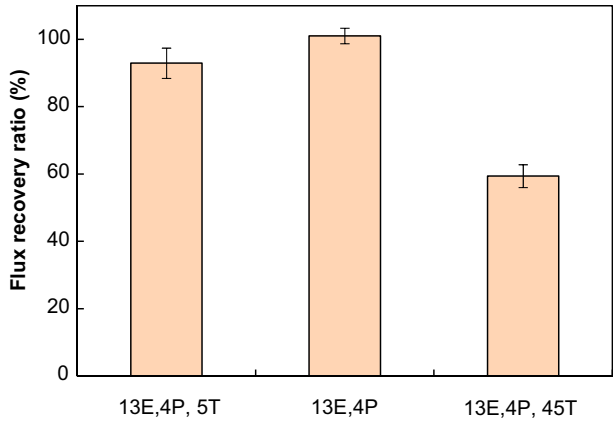

Fig. 16. FRR of the "13E, 4P" membranes prepared in various CBT after BSA fouling.

caused by more PEG leaching [43]. The FRR value of the "13E, 4P, 5T" membrane is 93% and it was attributed to the hydrophilicity of the membrane. Based on water contact angle, the hydrophilicity of "13E, 4P, 5T" membrane is lower than "13E, 4P" membrane.

Generally, performance tests showed that the "13E, 4P" membrane has the best efficiency. The parameters which led to introduce "13E, 4P" membrane as the best membrane among the fabricated membranes were the lowest flux decline, the high PWF, and the best FRR.

4. Conclusion

EPVC ultrafiltration membrane was improved by adding PEG as a pore former and hydrophilic additive. The addition of PEG to EPVC resulted in increasing hydrophilicity up to optimum concentration, and then in decreasing it. The results demonstrated that, in 13 wt.% EPVC, the PWF increased with increasing PEG concentration, but, in 15 wt.% EPVC, the trend was vice versa. The permeability of membranes was dependent on the concentration of PEG and EPVC in the casting solution. The SEM images illustrated that the prepared membranes possessed a finger-like structure. Antifouling experiments, using BSA filtration, indicated that the two parameters of hydrophilicity and pore size determine the antifouling properties of the membranes. The best antifouling membrane against protein fouling should have the highest hydrophilicity and should have the most finger-like structure in its surface. Investigating the effects of different CBT on morphology and performance showed that the membranes fabricated in high CBT have a higher PWF, but its antifouling properties were poor.

References

[1] K. Zodrow, L. Brunet, S. Mahendra, D. Li, A. Zhang, Q. Li, P.J.J. Alvarez, Polysulfone ultrafiltration membranes impregnated with silver nanoparticles show improved biofouling resistance and virus removal, Water Res. 43 (2009) 715–723.

[2] M. Sivakumar, D.R. Mohan, R. Rangarajan, Studies on cellulose acetate–polysulfone ultrafiltration membranes: II. Effect of additive concentration, J. Membr. Sci. 268 (2006) 208–219.

[3] A. Nabe, E. Staude, G. Belfort, Surface modification of polysulfone ultrafiltration membranes and fouling by BSA solutions, J. Membr. Sci. 133 (1997) 57–72.

[4] H. Susanto, M. Ulbricht, Characteristics, performance and stability of polyethersulfone ultrafiltration membranes prepared by phase separation method using different macromolecular additives, J. Membr. Sci. 327 (2009) 125–135.

[5] A. Rahimpour, S.S. Madaeni, A.H. Taheri, Y. Mansourpanah, Coupling TiO_2 nanoparticles with UV irradiation for modification of polyethersulfone ultrafiltration membranes, J. Membr. Sci. 313 (2008) 158–169.

[6] A. Rahimpour, S.S. Madaeni, Y. Mansourpanah, The effect of anionic, non-ionic and cationic surfactants on morphology and performance of polyethersulfone ultrafiltration membranes for milk concentration, J. Membr. Sci. 296 (2007) 110–121.

[7] M. Khayet, C.Y. Feng, T. Matsuura, Morphological study of fluorinated asymmetric polyetherimide ultrafiltration membranes by surface modifying macromolecules, J. Membr. Sci. 213 (2003) 159–180.

[8] L. Yan, Y.S. Li, C.B. Xiang, Preparation of poly(vinylidene fluoride) (pvdf) ultrafiltration membrane modified by nano-sized alumina (Al_2O_3) and its antifouling research, Polymer 46 (2005) 7701–7706.

[9] M. Khayet, C.Y. Feng, K.C. Khulbe, T. Matsuura, Preparation and characterization of polyvinylidene fluoride hollow fiber membranes for ultrafiltration, Polymer 43 (2002) 3879–3890.

[10] D. Wang, K. Li, W.K. Teo, Preparation and characterization of polyvinylidene fluoride (PVDF) hollow fiber membranes, J. Membr. Sci. 163 (1999) 211–220.

[11] K. Nouzaki, M. Nagata, J. Arai, Y. Idemoto, N. Koura, H. Yanagishita, H. Negishi, D. Kitamoto, T. Ikegami, K. Haraya, Preparation of polyacrylonitrile ultrafiltration membranes for wastewater treatment, Desalination 144 (2002) 53–59.

[12] X. Chai, T. Kobayashi, N. Fujii, Ultrasound effect on cross-flow filtration of polyacrylonitrile ultrafiltration membranes, J. Membr. Sci. 148 (1998) 129–135.

[13] L.I. Nass, Encyclopedia of PVC: Compounding Processes, Product Design, and Specifications, CRC Press, New York, NY, 1992.

[14] H. Rabiee, M.H.D.A. Farahani, V. Vatanpour, Preparation and characterization of emulsion poly(vinyl chloride)(EPVC)/TiO_2 nanocomposite ultrafiltration membrane, J. Membr. Sci. 472 (2014) 185–193.

[15] E.M. El-Nesr, A.M. Dessouki, E.M. Abdel-Bary, Gamma radiation induced graft copolymerization of acrylamide onto poly(vinyl chloride) films, Polym. Int. 46 (1998) 150–156.

[16] M.L. Yeow, Y.T. Liu, K. Li, Isothermal phase diagrams and phase-inversion behavior of poly(vinylidene fluoride)/solvents/additives/water systems, J. Appl. Polym. Sci. 90 (2003) 2150–2155.
[17] D. Wang, K. Li, W.K. Teo, Porous PVDF asymmetric hollow fiber membranes prepared with the use of small molecular additives, J. Membr. Sci. 178 (2000) 13–23.
[18] Z.L. Xu, F.A. Qusay, Polyethersulfone (PES) hollow fiber ultrafiltration membranes prepared by PES/non-solvent/NMP solution, J. Membr. Sci. 233 (2004) 101–111.
[19] A. Bottino, G. Capannelli, V. D'asti, P. Piaggio, Preparation and properties of novel organic–inorganic porous membranes, Sep. Purif. Technol. 22–23 (2001) 269–275.
[20] J. Xu, Z.L. Xu, Poly(vinyl chloride) (PVC) hollow fiber ultrafiltration membranes prepared from PVC/additives/solvent, J. Membr. Sci. 208 (2002) 203–212.
[21] H. Okuno, K. Renzo, T. Uragami, Influence of casting solution additive, degree of polymerization, and polymer concentration on poly(vinyl chloride) membrane properties and performance, J. Membr. Sci. 83 (1993) 199–209.
[22] M. Bodzek, K. Konieczny, The influence of molecular mass of poly(vinyl chloride) on the structure and transport characteristics of ultrafiltration membranes, J. Membr. Sci. 61 (1991) 131–156.
[23] S. Hirose, E. Yasukawa, T. Nose, Wet poly(vinyl chloride) membrane, J. Appl. Polym. Sci. 26 (1981) 1039–1048.
[24] F. Vigo, M. Nicchia, C. Uliana, Poly(vinyl chloride) ultrafiltration membranes modified by high frequency discharge treatment, J. Membr. Sci. 36 (1988) 187–199.
[25] Y. Peng, Y. Sui, Compatibility research on PVC/PVB blended membranes, Desalination 196 (2006) 13–21.
[26] P.R. Babu, V.G. Gaikar, Preparation, structure, and transport properties of ultrafiltration membranes of poly(vinyl chloride) (PVC), carboxylated poly(vinyl chloride) (CPVC), and PVC/CPVC blends, J. Appl. Polym. Sci. 73 (1999) 1117–1130.
[27] S. Mei, C. Xiao, X. Hu, Preparation of porous PVC membrane via a phase inversion method from PVC/DMAc/water/additives, J. Appl. Polym. Sci. 120 (2011) 557–562.
[28] S.S. Madaeni, S. Zinadini, V. Vatanpour, A new approach to improve antifouling property of PVDF membrane using *in situ* polymerization of PAA functionalized TiO_2 nanoparticles, J. Membr. Sci. 380 (2011) 155–162.
[29] J.F. Li, Z.L. Xu, H. Yang, L.Y. Yu, M. Liu, Effect of TiO_2 nanoparticles on the surface morphology and performance of microporous PES membrane, Appl. Surf. Sci. 255 (2009) 4725–4732.
[30] I.M. Wienk, R.M. Boom, M.A.M. Beerlage, A.M.W. Bulte, C.A. Smolders, H. Strathmann, Recent advances in the formation of phase inversion membranes made from amorphous or semi-crystalline polymers, J. Membr. Sci. 113 (1996) 361–371.
[31] R.M. Boom, I.M. Wienk, T. Van den Boomgaard, C.A. Smolders, Microstructures in phase inversion membranes. Part 2. The role of a polymeric additive, J. Membr. Sci. 73 (1992) 277–292.
[32] J.H. Kim, K.H. Lee, Effect of PEG additive on membrane formation by phase inversion, J. Membr. Sci. 138 (1998) 153–163.
[33] R.E. Kesting, The four tiers of structure in integrally skinned phase inversion membranes and their relevance to the various separation regimes, J. Appl. Polym. Sci. 41 (1990) 2739–2752.
[34] Z. Zhenxin, T. Matsuura, Discussions on the formation mechanism of surface pores in reverse osmosis, ultrafiltration, and microfiltration membranes prepared by phase inversion process, J. Colloid Interface Sci. 147 (1991) 307–315.
[35] C.A. Smolders, A.J. Reuvers, R.M. Boom, I.M. Wienk, Microstructures in phase-inversion membranes. Part 1. Formation of macrovoids, J. Membr. Sci. 73 (1992) 259–275.
[36] T. Mohammadi, E. Saljoughi, Effect of production conditions on morphology and permeability of asymmetric cellulose acetate membranes, Desalination 243 (2009) 1–7.
[37] W.Y. Chuang, T.H. Young, W.Y. Chiu, The effect of acetic acid on the structure and filtration properties of poly(vinyl alcohol) membranes, J. Membr. Sci. 172 (2000) 241–251.
[38] M.H.V. Mulder, Basic Principles of Membrane Technology, Kluwer Academic, Dordrecht, 1991.
[39] A. Idris, N.M. Zain, M.Y. Noordin, Synthesis, characterization and performance of asymmetric polyethersulfone (PES) ultrafiltration membranes with polyethylene glycol of different molecular weights as additives, Desalination 207 (2007) 324–339.
[40] D. Rana, T. Matsuura, Surface modifications for antifouling membranes, Chem. Rev. 110 (2010) 2448–2471.
[41] S. Zinadini, A.A. Zinatizadeh, M. Rahimi, V. Vatanpour, H. Zangeneh, Preparation of a novel antifouling mixed matrix PES membrane by embedding graphene oxide nanoplates, J. Membr. Sci. 453 (2014) 292–301.
[42] B. Jung, J.K. Yoon, B. Kim, H.W. Rhee, Effect of molecular weight of polymeric additives on formation, permeation properties and hypochlorite treatment of asymmetric polyacrylonitrile membranes, J. Membr. Sci. 243 (2004) 45–57.
[43] E. Saljoughi, M. Amirilargani, T. Mohammadi, Effect of PEG additive and coagulation bath temperature on the morphology, permeability and thermal/chemical stability of asymmetric CA membranes, Desalination 262 (2010) 72–78.